Supplementary information

Extending the π-Conjugated Benzoimidazoisoindolone-based n-Type Ladder Polymers: Highly Air-robust Aqueous Sodium-ion Electrochromic Energy Storage and Mechanism

Haolin Xie[a#], Jinming Zeng[a,*#]Zheng Xie[a], Yang Ou[a], Qingqing Qiu[a], Huan Li[a], Huiling Liu[a,c], Putrakumar Balla[d], Junyi Wu[a], Ping Liu[b], Tongxiang Liang[a]

[a] *College of Rare Earths, Jiangxi University of Science and Technology, Ganzhou 341000, PR China*
[b] *State Key Laboratory of Luminescent Materials and Devices, South China University of Technology, Guangzhou 510640, PR China*
[c] *Nankang No.6 High School, Ganzhou, Jiangxi 341400, PR China*
[d] *Department of Chemical Engineering and Applied Chemistry, Chungnam National University, Daejeon, 34134, South Korea*
[#] *These authors contributed equally to this work and should be considered co-first authors.*

Table of Contents

Results and discussion

Figure S1. Film thickness

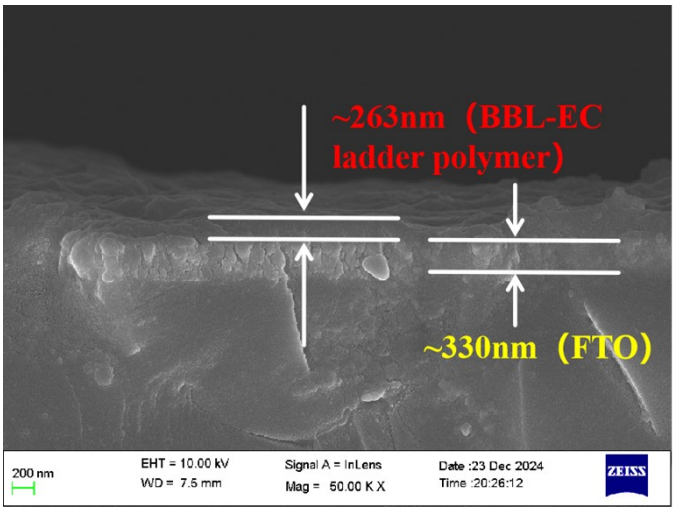

Figure S1. Film thickness of BBL-EC.

Figure S2. Absorption spectra

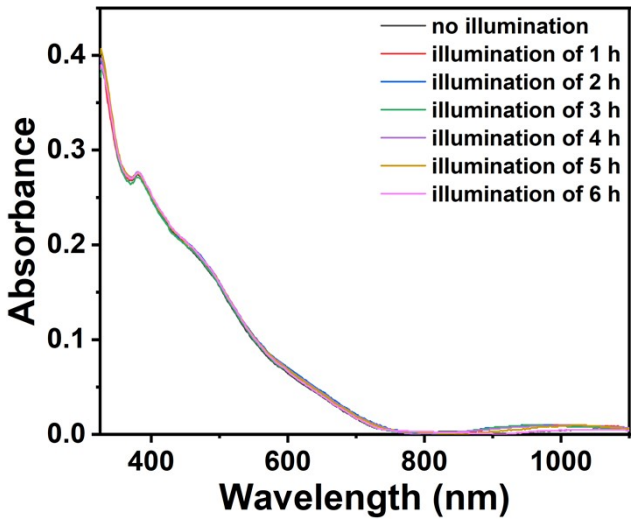

Figure S2. Absorption spectra of BBL-EC at different exposure times and in the air.

Figure S3. Raman spectra

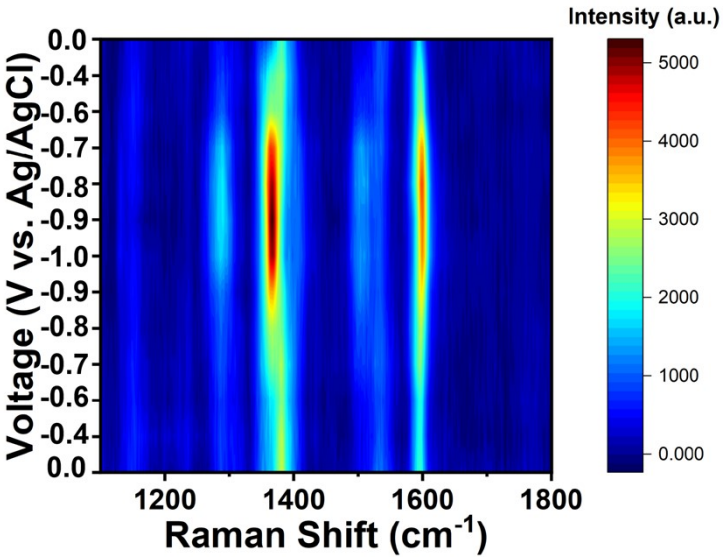

Figure S3. 2D mapping of the Raman spectra of BBL-EC.

Figure S4. Electron gain and loss mechanism

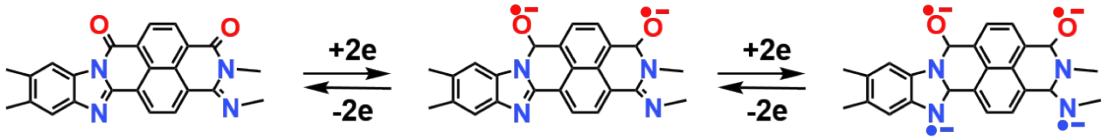

Figure S4. Electron gain and loss mechanism in electrochemical REDOX process of BBL-EC.

Figure S5. XPS spectra

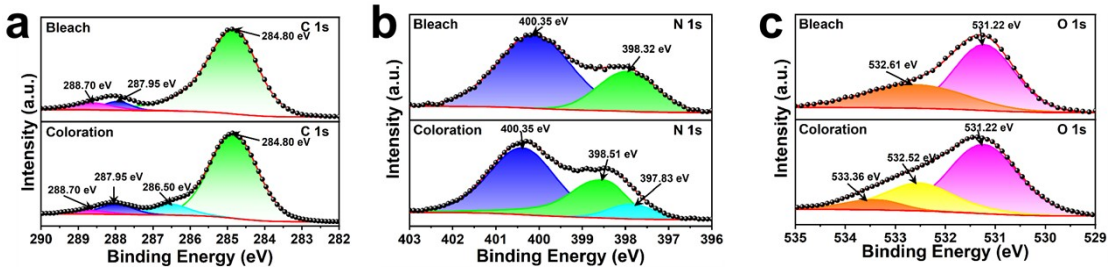

Figure S5. XPS (a) C 1s, (b) N 1s and (c) O 1s spectra of colored/bleached states of BBL-EC.

Figure S6. Plots of the j_p *vs.* $v^{1/2}$

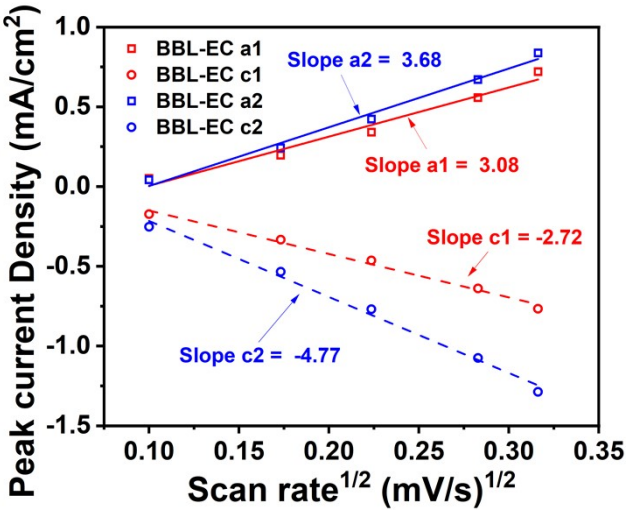

Figure S6. Plots of the j_p *vs.* $v^{1/2}$ of BBL-EC.

Figure S7. N_2 adsorption and desorption curves

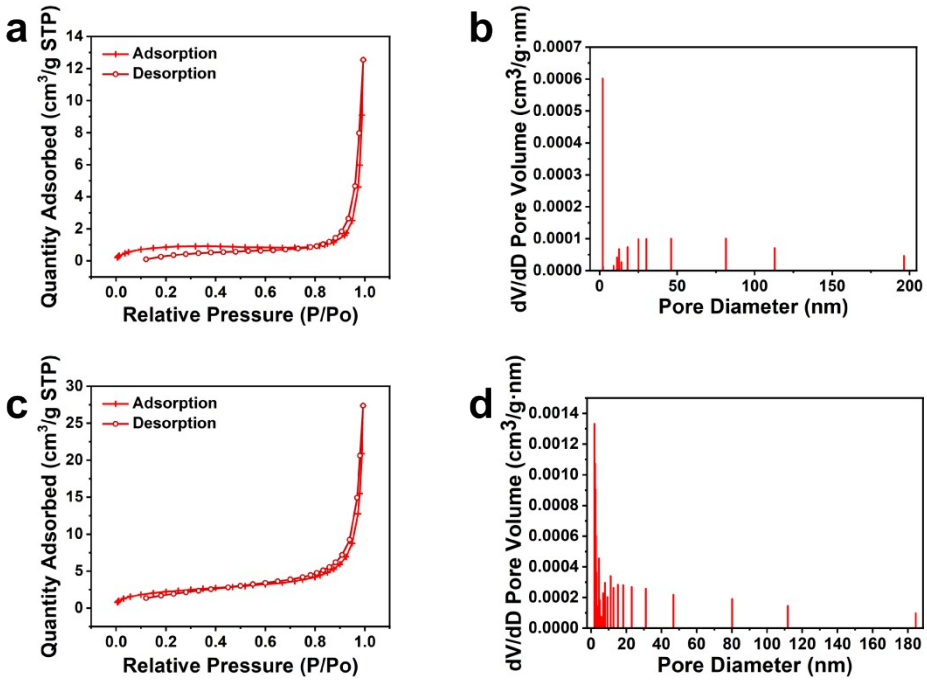

Figure S7. N_2 adsorption and desorption curves at 77K of (a) BBL-EC and (c) BAL-EC; Pore size distribution of (b) BBL-EC and (d) BAL-EC.

Figure S8. Electrochemical impedance spectroscopy (EIS)

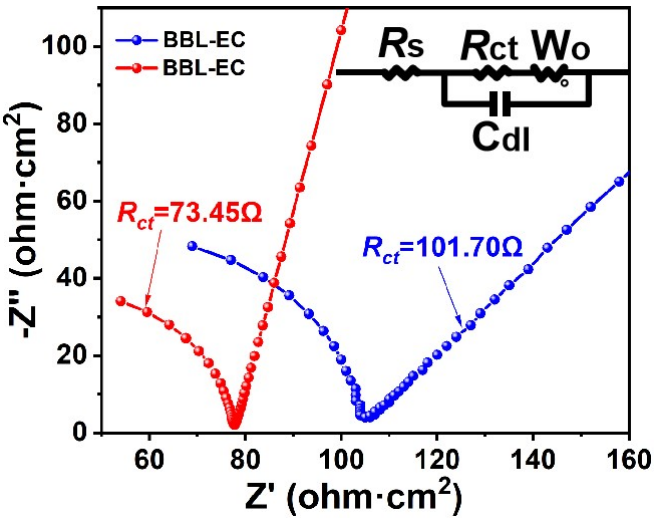

Figure S8. EIS (inset is equivalent circuit diagram) of BBL-EC and BAL-EC.

Figure S9. Electrochromic cycling stability of BBL-EC film

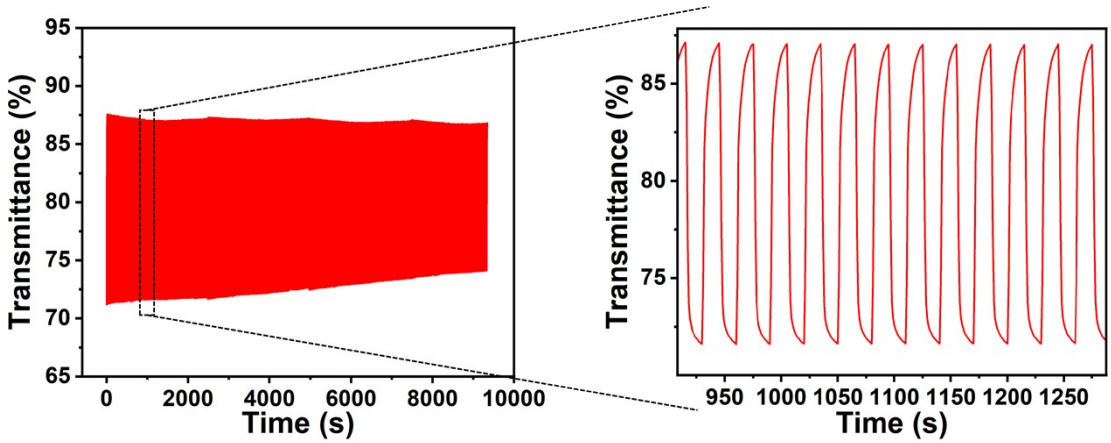

Figure S9. Electrochromic cycling stability of BBL-EC film.

Figure S10. GCD curves and specific capacity

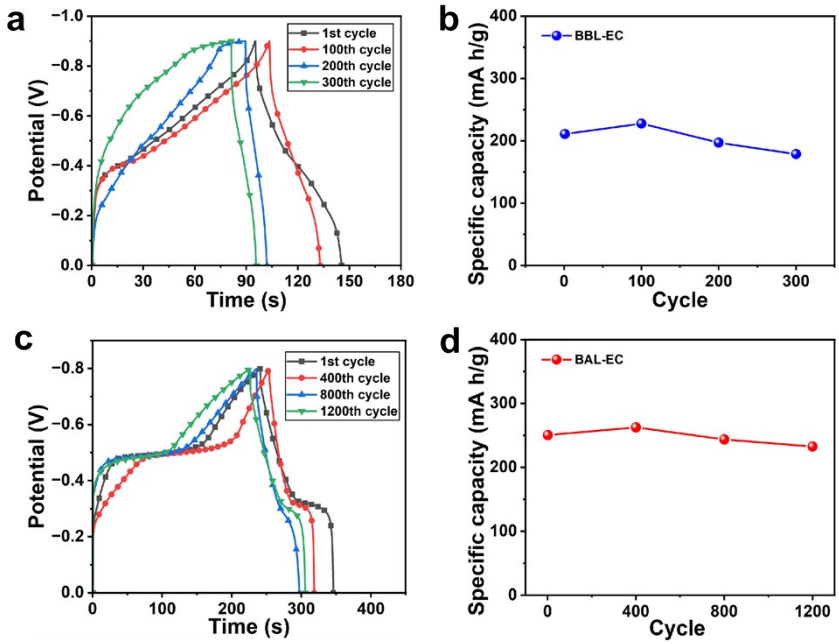

Figure S10. GCD curves and specific capacity of (a, b) BBL-EC and (c, d) BAL-EC at 0.3 mA/cm^2.

Figure S11. Electrochemical cycling stability under illumination conditions

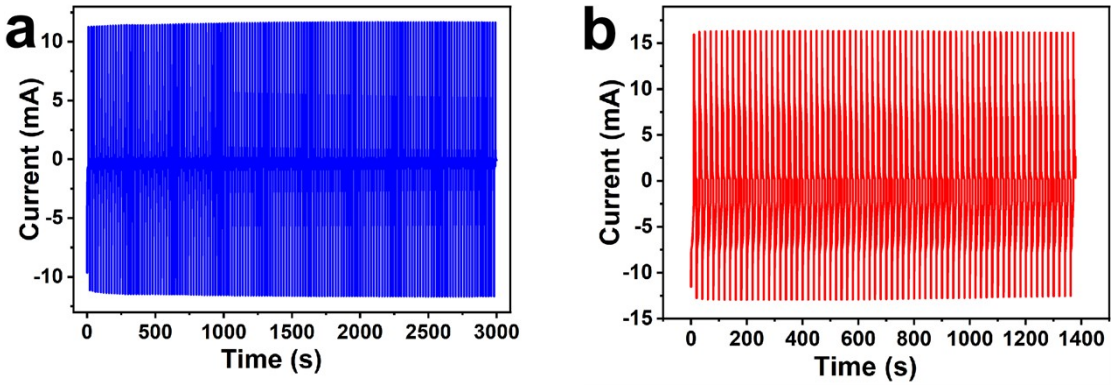

Figure S11. Electrochemical cycling stability of (a) BBL-EC and (b) BAL-EC under illumination conditions.

Figure S12. Electrochromic performance of BBL-EC at different temperatures

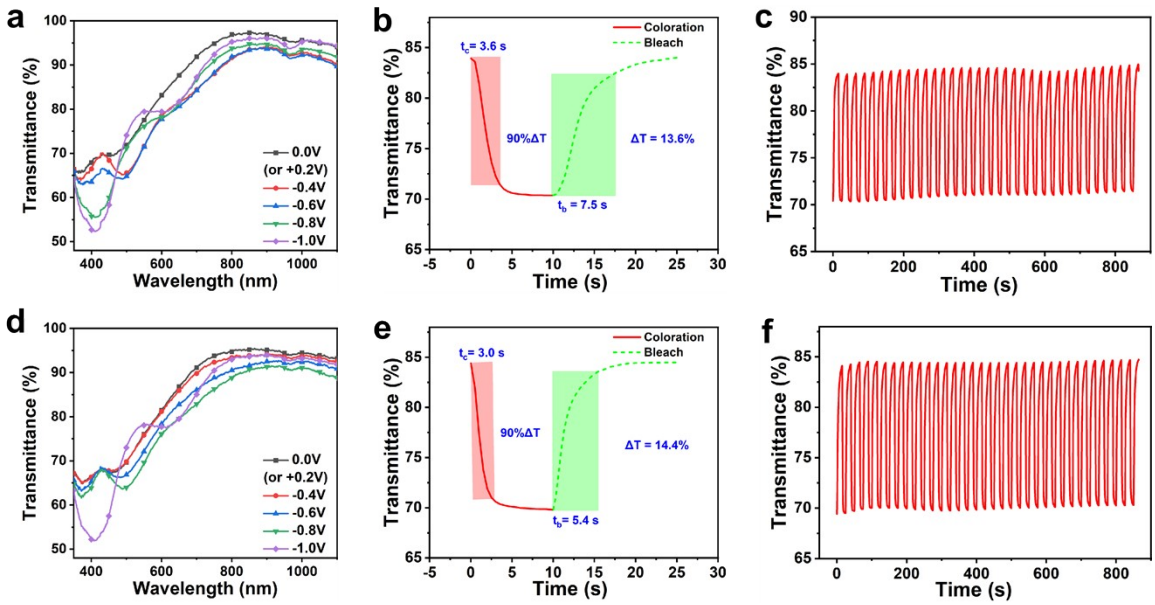

Figure S12. Electrochromic performance of BBL-EC at different temperatures. (a, d) Spectroelectrochemistry ; (b, e) response times; and (c, f) cycling stability tests at 0°C and 40°C.

Figure S13. Electrochromic performance of BAL-EC at different temperatures

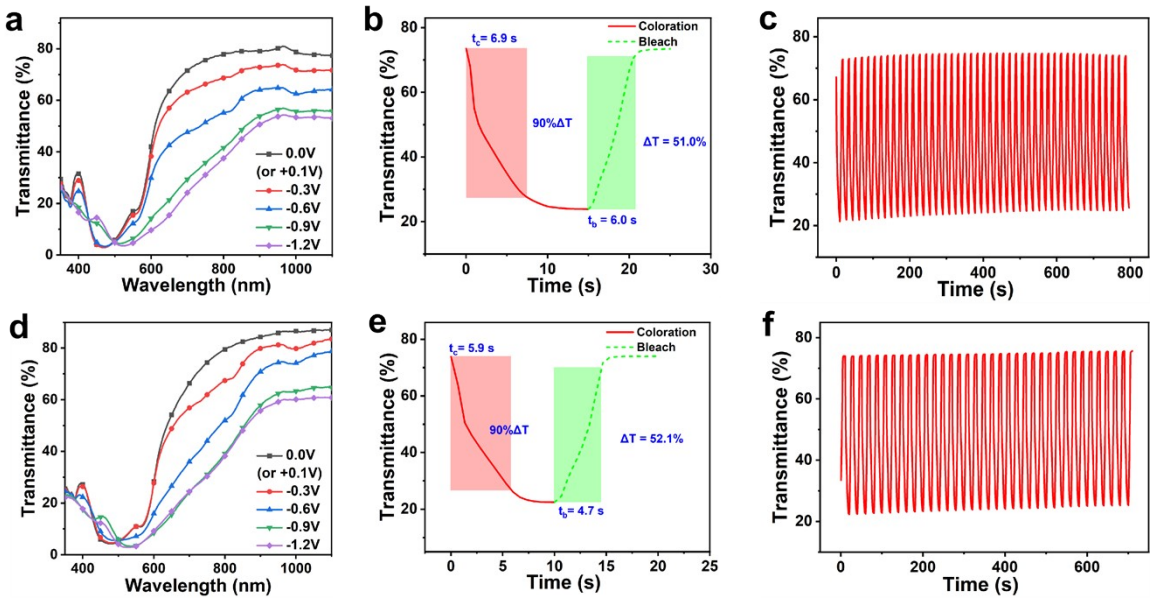

Figure S13. Electrochromic performance of BAL-EC at different temperatures. (a, d) Spectroelectrochemistry ; (b, e) response times; and (c, f) cycling stability tests at 0°C and 40°C.

Figure S14. Electrochromic performance of ECD

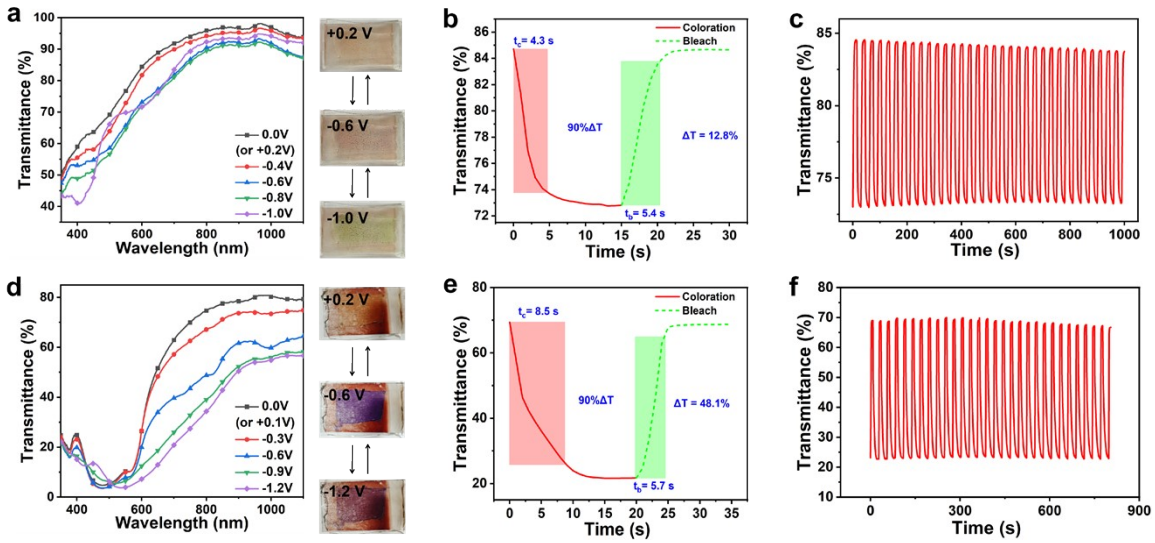

Figure S14. Comparison of the electrochromic performance of ECD-BBL and ECD-BAL. Spectroelectrochemistry and electrochromic digital photos, coloring/bleaching time and optical contrast, long-term cycling life of (a, b, c) ECD-BBL and (d, e, f) ECD-BAL.

Figure S15. GCD curves

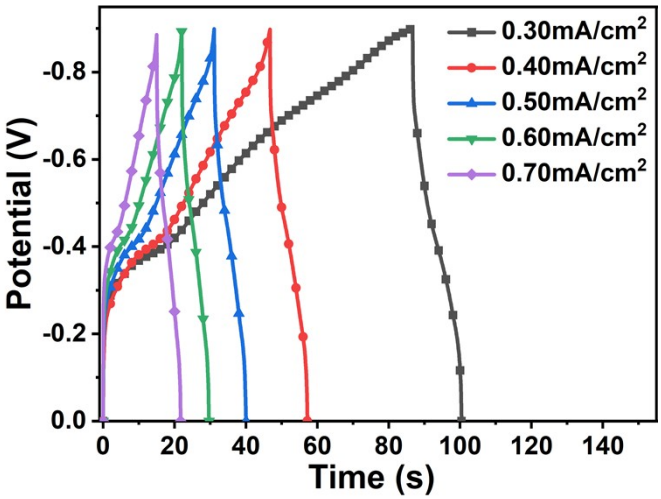

Figure S15. GCD curves of BBL-EC.

Figure S16. Raman spectra during the charge-discharge

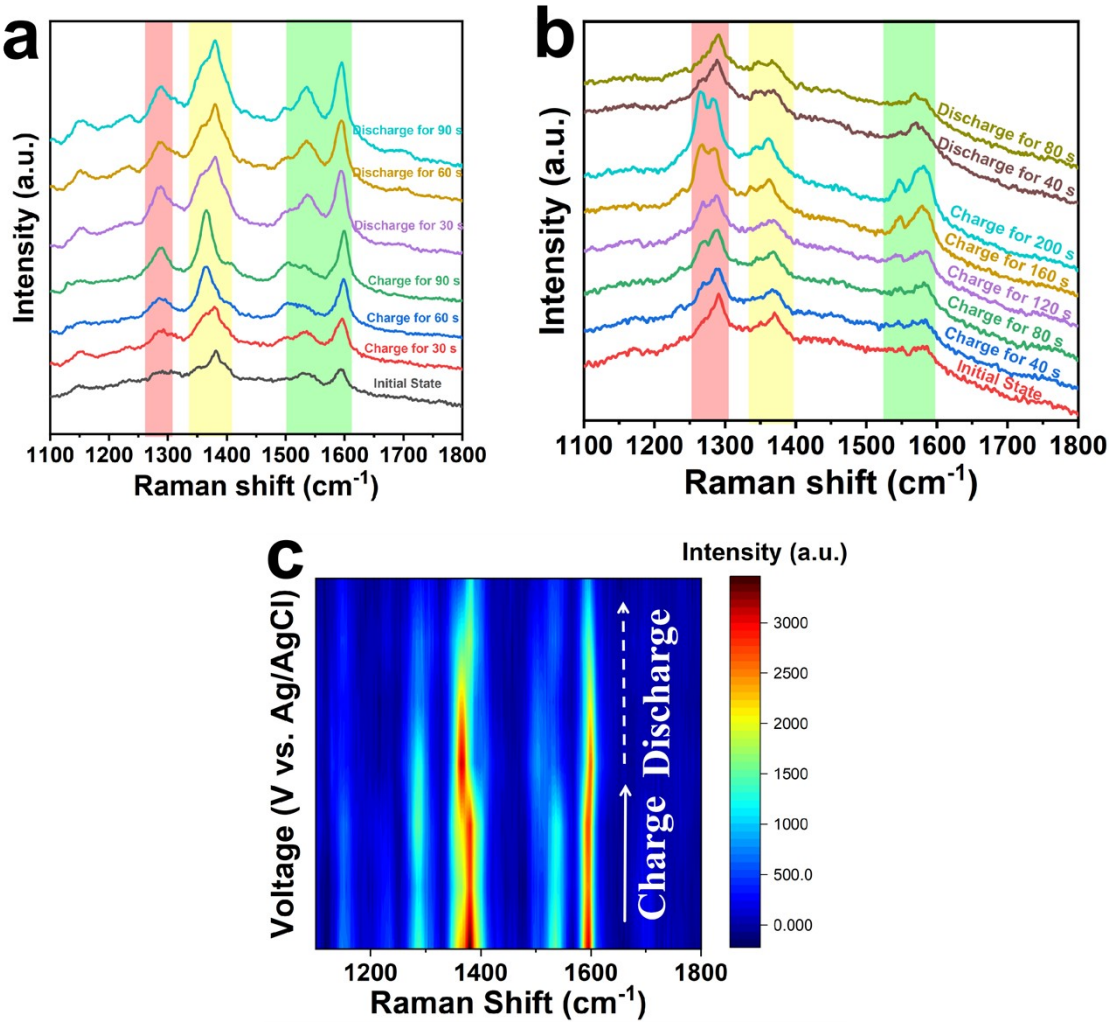

Figure S16.1D and 2D mapping of the Raman spectra during the charge-discharge process of (a, c) BBL-EC and (b)BAL-EC.

Figure S17. GCD curves and capacity retention

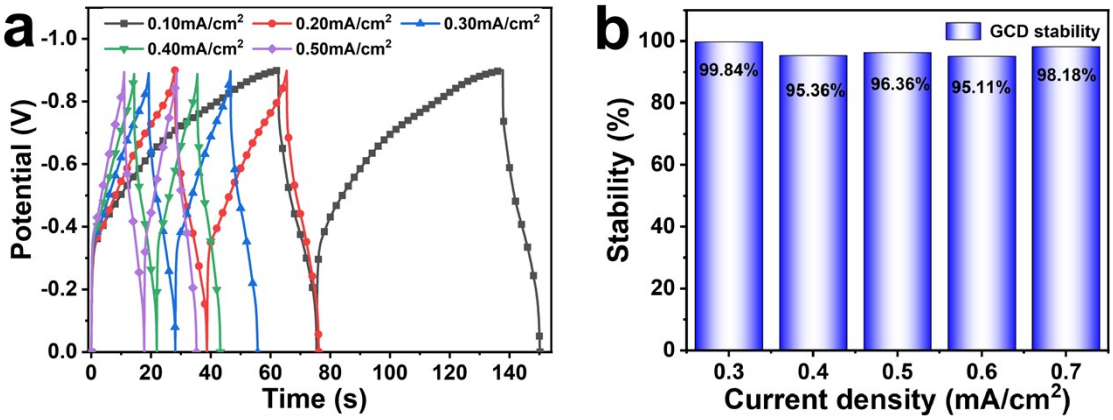

Figure S17. (a) GCD curves and (b) capacity retention of BBL-EC.

Table S1. Detailed fitting parameters of Nyquist plots for BBL-EC ladder polymer

Element	Value	Error	Error %
R_s	2.543	0.15558	6.118
R_{ct}	101.7	0.19682	0.19487
W_o-R	617	20.826	3.3715
W_o-T	0.09786	0.0068706	7.0208
W_o-P	0.56259	0.0029934	0.53207
C_{dl}	1.139×10^{-9}	1.0387×10^{-11}	0.91218

Table S2. Detailed fitting parameters of Nyquist plots for BAL-EC ladder polymer

Element	Value	Error	Error %
R_s	5.341	0.1219	2.2823
R_{ct}	73.45	0.12564	0.17414
W_o-R	0.0071394	2.2257×10^{-5}	0.31175
W_o-T	2.865×10^{-8}	1.0331×10^{-10}	0.36059
W_o-P	0.43228	0.00089009	0.20591
C_{dl}	1.545×10^{-9}	1.6486×10^{-11}	1.067

Table S3. Capacitive Performance of Electrochromic Polymers

EC films	Capacitance	Ref.
TPAB (n-type)	2.38 (mF cm^{-2})	[1]
PECE (p-type)	3.04 (mF cm^{-2})	[2]
PECE (p-type)	3.04 (mF cm^{-2})	
P(TPACz) (p-type)	0.433 (mF cm^{-2})	[3]
P(TPACz)/WO_3 (p-type)	1.94 (mF cm^{-2})	
WO_3@PANI (p-type)	147.8 (mF cm^{-2})	[4]
PM-TPI COF (p-type)	89.8 (mAh g^{-1})	[5]
NT-TPI COF (p-type)	141.0 (mAh g^{-1})	
TAPA-PMDA PI COF (p-type)	94.07 (mAh g^{-1})	[6]
TAPA-NTCDA PI COF (p-type)	86.57 (mAh g^{-1})	
PB/PPy-Zn (n-type)	109.9 (mAh g^{-1})	[7]
BBL-EC (n-type)	203.49 (mAh g^{-1})	This work
BAL-EC (n-type)	257.22 (mAh g^{-1})	This work

Ref. [1] P. N. Wang, S. Q. Zheng and B. P. Lin, J. *Solid State Electrochem.*, 2024, 28, 3781-3792.

Ref. [2] E. G. C. Ergun and A. M. Önal, *Electrochim. Acta*, 2025, 510, 145379.

Ref. [3] P. N. Wang, Y. Sun, J. Li, G. Q. Zhu, X. Q. Zhang, H. Yang and B. P. Lin, *J. Alloys Compd.*, 2022, 922, 166195.

Ref. [4] Y. Z. Meng, J. R. Yin, L. Y. Wang, X. J. Yang, X. S. Li and Y. Jiang, *Mater. Lett.*, 2023, 335, 133809.

Ref. [5] L. Huang, R. Guo, Q. Qiu, H. Li, P. Balla, J. Zeng, T. Liang, X. Qi and P. Liu, *Chem. Eng. J.*, 2024, 497, 155018.

Ref. [6] H. Xie, Q. Qiu, H. Li, P. Liu, P. Balla, X. Qi, T. Liang and J. Zeng, ACS Appl. *Mater. Interfaces*, 2024, 17, 2180-2189.

Ref. [7] Z. Xiang, Z. H. Li, X. J. Yang, Y. Yang, X. S. Li, Y. Gao, L. Y. Wang and W.

Lü, *Chem. Eng. J.*, 2025, 512, 162491.

Table S4. Performance Comparison Table of n- and p-Type Electrochromic Energy Storage Materials

EC films	ΔT (%)	t_b/t_c [a)](s)	CE (cm^2/C)	Electrolyte	Cyclic Stability	Capacitance	Ref.
pPMQT	32.20 (490 nm)	2.1/1.7	116.52	$Zn(TfO)_2$	-	217.13 (mAh g^{-1})	[8]
pNTQT	38.49 (474 nm)	2.4/1.8	182.86	$Zn(TfO)_2$	-	349.79 (mAh g^{-1})	[8]
TPAB	9 (654 nm)	6.49/7.03	41.81	$LiClO_4$/PC	-	2.23 (mF cm^{-2})	[1]
TPANB	10 (680 nm)	3/4	36.19	$LiClO_4$/PC	-	2.13 (mF cm^{-2})	[1]
ALV-BF_4_X	25	4.03/3.45	56	$LiClO_4$/ACN	Retain 56% (after 100 cycles)	1.713×10^{-4} (F cm^{-2})	[9]
ALV-ClO_4_X	29	2.84/0.53	82	$LiClO_4$/ACN	Retain 72% (after 100 cycles)	1.538×10^{-4} (F cm^{-2})	[9]
ALV-PF_6_X	25	3.14/3.02	58	$LiClO_4$/ACN	Retain 83% (after 100 cycles)	2.499×10^{-4} (F cm^{-2})	[9]
ALV-TFSI_X	22	3.53/3.76	77	$LiClO_4$/ACN	Retain 80% (after 100 cycles)	8.94×10^{-4} (F cm^{-2})	[9]
BBL	30	-/21	-	Drinking Water	Retain 90% (after 1000 cycles)	-	[10]
ProDOT-Am	-	2/＞10	-	NH_4Cl/H_2O	Retain 60% (after 100 cycles)	-	[11]
LPANI	-	0.1/0.39	-	PMMA/PC /LiClO	Retain 98% (after 200 cycles)	-	[12]
BBL@CNT	-	-	-	H_2/H_2O	Retain 99.7% (after 500 cycles)	268 (mAh g^{-1})	[13]
BAL-EC	53.8 (740 nm)	6.4/6.2	20.62	$NaCl/H_2O$	No obvious ΔT% drop (after 1200 cycles)	257.22 (mAh g^{-1})	This work

a) t_c: coloring time, t_b: bleaching time.

Ref. [8] Z. X. Liu, Y. Li, B. H. Mei, J. X. Liu, H. J. Niu and Y. J. Hou, *Int. J. Mol. Sci.*, 2025, 26, 3838.

Ref. [9] S. Ulucay, N. G. Ha, A. Kortun, S. Altinisik, S. Piravadili, J. H. Kwon, H. C. Moon and S. Koyuncu, *Org. Electron.*, 2025, 144, 107273.

Ref. [10] Y. Z. Tian, Z. Q. Lu, Z. Y. Bai, H. Li, Y. Y. Hao, Q. H. Zhang, Y. G. Li, C. Y. Hou, K. R. Li and H. Z. Wang, *Chem. Eng. J.*, 2025, 519, 165141.

Ref. [11]K. Perera, Z. Yi, L. You, Z. Ke, J. Mei, *Polym. Chem.,* 2020, **11**, 508-516.

Ref. [12]X.Z. Ji, M.W. Leng, H.M. Xie, C.X. Wang, K.R. Dunbar, Y. Zou, L. Fang, *Chem. Sci.,* 2020, **11**, 12737-12745.

Ref. [13]T. Ma, Y. Yang, D. Johnson, K. Hansen, S. Xiang, R.M. Thakur, A. Djire, J.L. Lutkenhaus, *Joule,* 2023, **7**, 2261-2273.